30-year mesoscale model simulations for the “Noise from wind turbines and risk of cardiovascular disease” project

Pena Diaz, Alfredo; Hahmann, Andrea N.

Publication date:
2017

Document Version
Publisher's PDF, also known as Version of record

30-year mesoscale model simulations for the "Noise from wind turbines and risk of cardiovascular disease" project

DTU Wind Energy E-Report

Alfredo Peña and Andrea N. Hahmann

DTU Wind Energy-E-Report-0055(EN)
February 2017

DTU Wind Energy
Department of Wind Energy

DTU Wind Energy Report-E-0055(EN)

30-year mesoscale model simulations for the "Noise from wind turbines and risk of cardiovascular disease" project

Alfredo Peña and Andrea N. Hahmann

DTU Wind Energy
Department of Wind Energy

DTU Wind Energy, Risø Campus,
Technical University of Denmark, Roskilde, Denmark

February 2017

Author: Alfredo Peña and Andrea N. Hahmann
Title: 30-year mesoscale model simulations for the "Noise from wind turbines and risk of cardiovascular disease" project
Department: DTU Wind Energy

DTU Wind Energy
Report-E-0055(EN)
February 13, 2017

ISSN:
ISBN:
978-87-93896-95-7

Abstract (max. 2000 char)

This report documents the work performed by DTU Wind Energy for the project "Noise from wind turbines and risk of cardiovascular disease" lead by the Danish Cancer Society (Kræftens Bekæmpelse). The aim of the project is to investigate if exposure to wind turbine noise can be associated with and increased risk for cardiovascular disease by using Danish health-like registers.
DTU Wind Energy produced a 30-year mesoscale model simulation, which was used to extract wind and other meteorological parameters at 7773 turbine site locations in the whole Denmark. The data extracted were delivered to Kræftens Bekæmpelse and are used by the Danish Electronics, Light & Acoustics (DELTA) to perform noise estimations at sites nearby the turbine locations.
Here we describe the mesoscale model used for the simulations, the setup of the simulation, and how the extraction of the data was performed. Finally, a comparison of simulated model outputs with observations from a high-quality meteorological mast is also provided.

Contract no:

Project no:

Sponsorship:
The Danish Ministry of Environment and the Danish Ministry of Climate, Energy and Building

Cover:

Pages: 25
Tables: 3
Figures: 17
References: 18

Technical University of Denmark
Frederiksborgvej 399
4000 Roskilde
Denmark
Tel. +4546775024
aldi@dtu.dk
www.vindenergi.dk

Contents

1 Introduction

In September 2013, the Danish Cancer Society (Kræftens Bekæmpelse–KB) leaded an application to the Danish Ministry of Environment and the Danish Ministry of Climate, Energy, and Building related to the study of the effect of noise from wind turbines and the risk of cardiovascular disease within the last 30 years in the entire Denmark. For such a study, historical time series of meteorological (met) parameters, such as wind speed and direction, are needed in order to estimate the noise from the wind turbines. KB approached DTU Wind Energy to figure out if such a collection of historical data exists. Some met and weather stations in Denmark have records covering the last $\approx$50 years but they are relatively few stations (thousands of turbines have been installed in Denmark covering all territories) and the observations are performed close to the ground (typically at 10 m above mean sea level; all heights are hereafter refer to this level) and most wind turbines are placed at much higher heights.

One relatively "inexpensive" way to provide such data is by using reanalysis datasets. However the latter provide met data over spatial grids which are relatively too coarse and with too low frequency; KB was looking at studying all residential spots close to all registered wind turbines in Denmark, which account for $\approx$7773 machines. DTU Wind Energy suggested to use a mesoscale model to simulate the atmosphere in the entire Denmark for the last 30 years and to use such model to extract the necessary met outputs at all turbine sites in the whole Denmark. Such simulations would become the longest and heaviest mesoscale runs performed at DTU Wind Energy.

The simulations started in the new DTU computer cluster in April 2014 and finished in July 2014. Data at 7773 turbine sites were extracted and delivered to KB in August 2014. Here, we provide a detailed description of the mesoscale model used, including its setup for the particular simulations, a description of the data extracted, and the evaluation of the simulation outputs by using the high-quality met mast DTU Wind Energy has maintained for more than 10 years at the National Station for Wind Turbines located in Høvsøre, Denmark.

2 The mesoscale model

2.1 Overview

The data delivered within this project was produced using the Weather, Research and Forecasting (WRF) Model (`http://www.wrf-model.org`). The WRF model is a mesoscale numerical weather prediction system designed to serve both operational forecasting and atmospheric research needs. The WRF model can generate atmospheric simulations using real data (observations, analyses) or idealized conditions. WRF offers operational forecasting a flexible and computationally-efficient platform while providing recent advances in physics, numerics, and data assimilation contributed by developers across the very broad research community.

The simulations used here utilize the Advanced Research WRF (ARW-WRF) version 3.5.1 model released on 23 September 2013. The WRF modeling system is in the public domain and is freely available for community use. It is designed to be a flexible, state-of-the-art atmospheric simulation system that is portable and efficient on available parallel computing platforms. The WRF model is used worldwide for a variety of applications, from real-time weather forecasting, regional climate modeling, to simulating small-scale thunderstorms.

Although designed primarily for weather forecasting applications, ease of use and quality has brought the WRF model to be the model of choice for downscaling in wind energy applications. Offshore, the method has been validated over the North and Baltic Seas in Hahmann and Peña (2010) and over land for South Africa in Hahmann et al. (2014).

2.2 Model setup

The simulations were integrated on a grid with horizontal spacing of 18 km $\times$ 18 km (outer domain, D1, with 121 $\times$ 87 grid points), 6 km $\times$ 6 km (first nested domain, D2, with 280 $\times$ 178 grid points) and 2 km $\times$ 2 km (second nest, D3, with 427 $\times$ 304 grid points). A map of the model setup location, which was rotated to better cover the region of interest over Denmark, Sweden, and Northern Germany, is displayed in Fig. 1.

The simulations use 41 vertical levels from the surface to a height of approximately 20 km. The levels are closer together near the Earth surface to better simulate the exchanges of heat and momentum between the surface and the atmosphere. The lowest 12 of these levels are within 1000 m of the surface and the first level is located at approximately 14 m AGL. Table 1 list the details of the model configuration, including the model parametrizations used in the simulations.

Most choices in the model setup are fairly standard and used by other modeling groups. The only special setting for wind energy applications is the use of a constant surface roughness length, thus disabling the annual cycle available in the WRF model.

The simulation covered the 32 year period 1982–2013 (to be extended to 2015), and was run in a series of 11-day long overlapping simulations, with the output from the first day being discarded. This method is based on the assumptions described in Hahmann et al. (2010). The simulation used grid nudging that continuously relaxes the model solution towards the gridded reanalysis but this was done only on the outer domain and above the boundary layer (level 10 from the surface) to allow for the mesoscale processes near the surface to develop freely. Because the simulations were re-initialized every 10 days, the runs are independent of each other and can be integrated in parallel reducing the total time needed to complete a multi-year climatology. The grid nudging and 10-days reinitialization keep the model solution from drifting from the observed large-scale atmospheric patterns, while the relatively long simulations guarantee that the mesoscale flow is fully in equilibrium with the mesoscale characteristic of the terrain. One major change to the standard WRF modeling system was the change in landuse (and its associated surface roughness length). Detailed inspection of the standard landuse maps in WRF showed serious problems. Therefore, new types based on the work of Refslund et al. (2014) were used. See section 2.3.

Model setup:
WRF (ARW) Version 3.5.1.
Mother domain (D1; 121 $\times$ 87 grid points) with 18 km grid spacing; 2 nested domains: D2 (280 $\times$ 178 grid points) using 6 km and D3 (427 $\times$ 304 grid points) horizontal grid spacing on a polar stereographic projection (see Fig. 1).
41 vertical levels with model top at 50 hPa; 9 of these levels are placed within 1000 m of the surface; The first 6 levels are located approximately at: 14, 43, 72, 100, 129 and 190 m.
MODIS (2001–2010) land-cover classification of the International Geosphere-Biosphere Programme.
Changes to lakes for better representation of inland water bodies.
Simulation setup:
Initial, boundary conditions, and fields for grid nudging come from the European Centre for Medium Range Forecast (ECMWF) ERA-Interim Reanalysis (Dee et al., 2011) at $0.7^\circ \times 0.7^\circ$resolution.
Runs are started (cold start) at 00:00 UTC every 10 days and are integrated for 11 days, the first 24 hours of each simulation are disregarded.
Sea surface temperature (SST) and sea-ice fractions come from the dataset produced at USA NOAA/NCEP at $0.25^\circ \times 0.25^\circ$resolution (Reynolds et al., 2010) and are updated daily.
Model output: hourly (lowest 11 vertical levels) for D3, 3-hourly for D1 and D2, wind speeds at 7 vertical levels every 10 minutes for D3 only. Time step in most simulations: approx. 106 seconds.
One-way nested domains; 5 grid point nudging zone.
Spectral nudging on D1 only and above level 10; wavenumber 9 and 6 in the zonal and meridional direction. Nudging coefficient 0.0003 s^{-1} for wind, temperature and specific humidity. No nudging in the PBL.
Physical parameterizations:
Precipitation: WRF Single-Moment 5-class scheme (option 4), Kain-Fritsch cumulus parameterization (option 1) turned off on D3.
Radiation: RRTM scheme for longwave (option 1); Dudhia scheme for shortwave (option 1)
PBL and land surface: Yonsei University Scheme (YSU) scheme Hong et al. (2006) (option 1), MM5 similarity (option 1) surface-layer scheme, and Noah Land Surface Model (option 2).
Surface roughnesses are kept constant at their winter (lower) value.
Diffusion: Simple diffusion (option 1); 2D deformation (option 4); 6th order positive definite numerical diffusion (option 2); rates of 0.06, 0.08, and 0.1 for D1, D2, and D3, respectively; vertical damping.
Positive definite advection of moisture and scalars.

Table 1: Summary of model and system setup and physical parameterizations used in the simulations.

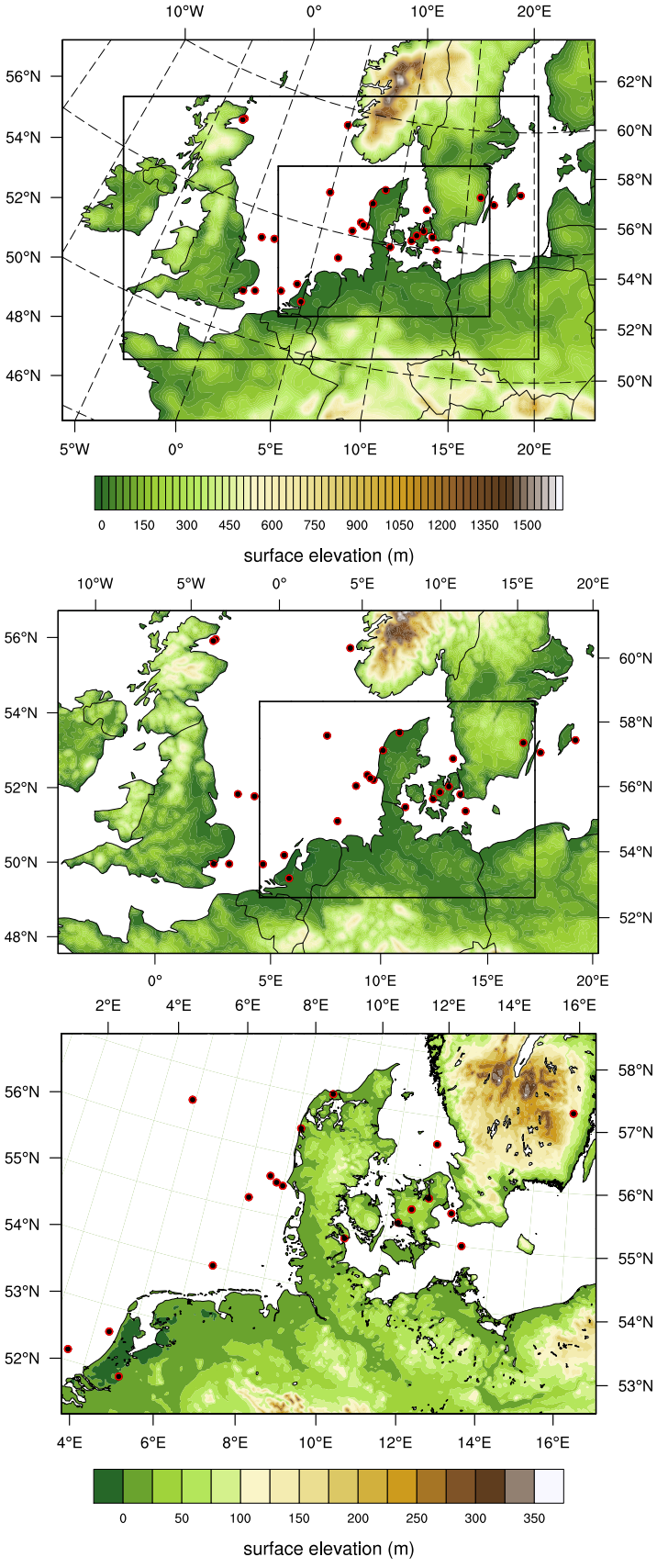

Figure 1: WRF model domains configuration and terrain elevation (m). Top left: 18 km $\times$ 18 km domain (D1), Top right: 6 km x 6 km (D2) and Bottom: 2 km $\times$ 2 km (D3). The inner lines show the position of D2 and D3 in D1 and D2, respectively. The location of wind measurement sites within the region is show by the dots.

2.3 Updated vegetation

From the MODIS product documentation[1] reports significant problems in the training data which may have serious consequences for the classified data. The document reports that overall previous versions of the MODIS-based data still overestimated forest cover in most areas. Newer versions of the dataset, such as the one used to generate the lower map in Fig. 2, show improvements over previous versions.

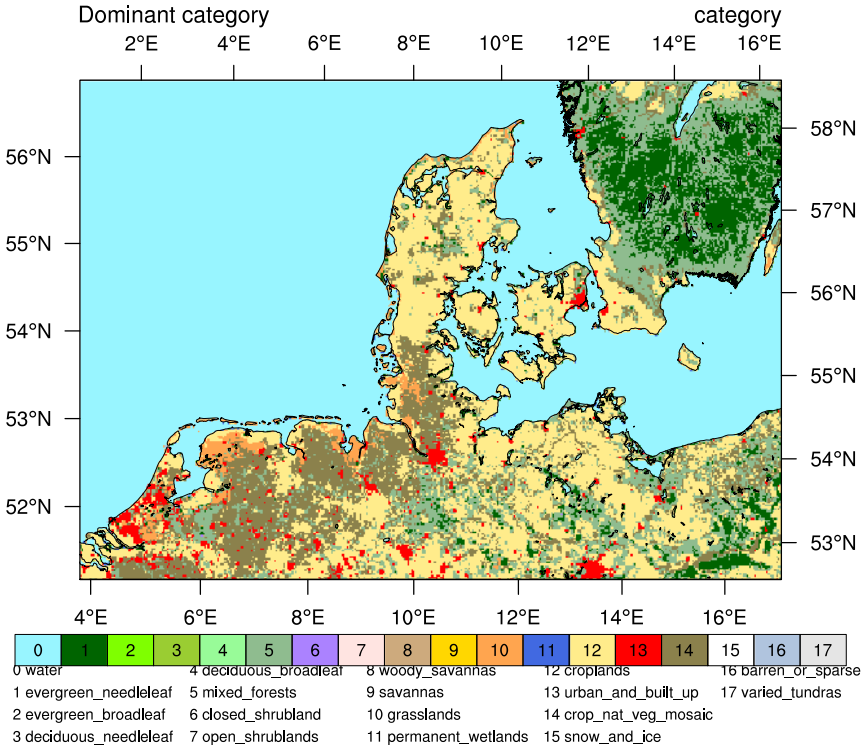

Figure 2: Land use categories for the WRF domain 3.

For the simulation we used an “averaged" landuse map for the period 2001–2010 derived from MODIS Collection 5 (Friedl et al., 2010), as opposed to the MODIS C4-based data from a single year for 2001 used in the default WRF V3.5.1.

Surface roughnesses were modified from those used in the standard WRF V3.5.1 setup. The new values are presented in Table 2. In addition to the new values, the annual variation in surface roughness used in WRF was disabled by setting the minimum and maximum values to a single value.

2.4 Simulation setup

2.5 Pre-evaluation and sensitivity experiments

We setup the model and simulations based on experience gained from different projects in which WRF has been used for both forecasting and climate studies (Draxl et al., 2014a; Hahmann and Peña, 2010). But one important recurrent issue is the choice of PBL scheme, as some might suit better certain conditions/sites and even the purpose of the simulations. We, therefore, tested three of the most known PBL schemes: the MYJ (PBL1), the MYNN (PBL2), and the YSU (PBL3) for 1 month, which has high variability for both winds and temperature (September 2013). As the

[1] http://daac.ornl.gov/MODIS/MODIS-menu/MCD12Q1_known_issues.html

MODIS Landuse class	Min/Max stand roughness (m)	New roughness (m)
Evergreen Broadleaf Forest	0.50/0.50	0.90
Mixed Forests	0.20/0.50	0.50
Grasslands	0.10/0.12	0.10
Croplands	0.05/0.15	0.10
Urban and Built-Up	0.50/0.50	0.50
Cropland/natural vegetation mosaic	0.05/0.14	0.10
Barren or Sparsely Vegetated	0.01/0.01	0.01
Barren tundra	0.05/0.10	0.075

Table 2: Surface roughness length as a function of landuse class for the standard WRF (minimum and maximum) and the modified for the DK-HR simulations.

domain of the simulations is rather large we choose a smaller grid for the pre-evaluation, which is shown in Fig. 3.

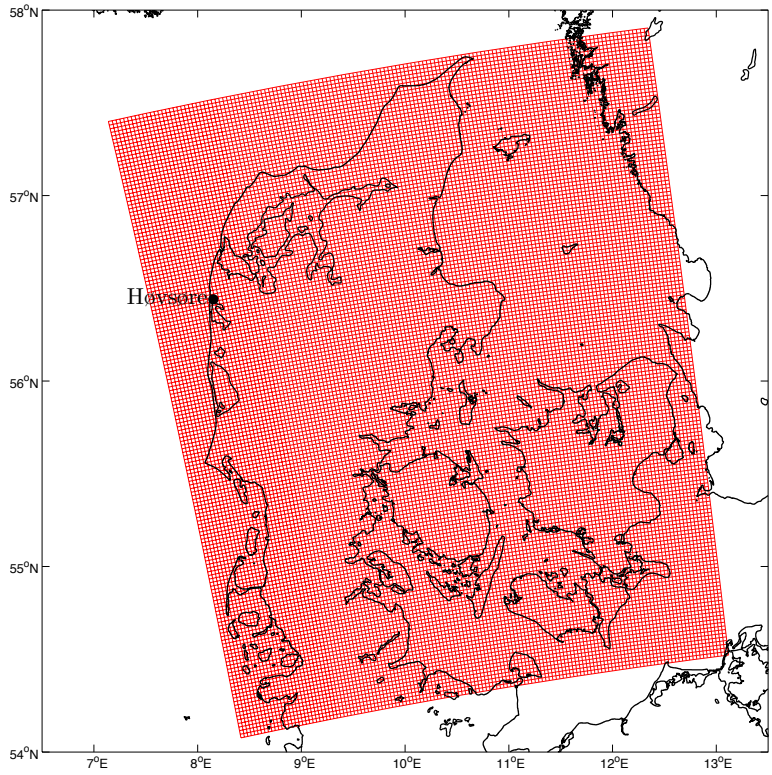

Figure 3: The 2-km mass grid of the WRF model setup used for the simulations (here limited to the are of Denmark without Bornholm). The location of the Høvsøre site is also displayed

As a first attempt for choosing the PBL scheme, we derive root mean square (RMS) differences between the 2D fields of wind speed and temperature at the fourth level ($\approx$ 100 m) of the three schemes. Figure 4 illustrates these RMS differences and, as shown, the RMS difference for the temperature field is highest between the MYNN and the PBL schemes, whereas for wind field it is between the MYJ and MYNN schemes. This very qualitatively means that the MYNN scheme is the one producing the highest differences. This does not mean that such scheme is worse than the others but for weather prediction purposes and the production of wind climatologies, one would like to find consistency in the resulting simulated fields even though the PBL schemes are different.

For September 2013 we can make use of measurements from a high-quality mast located in

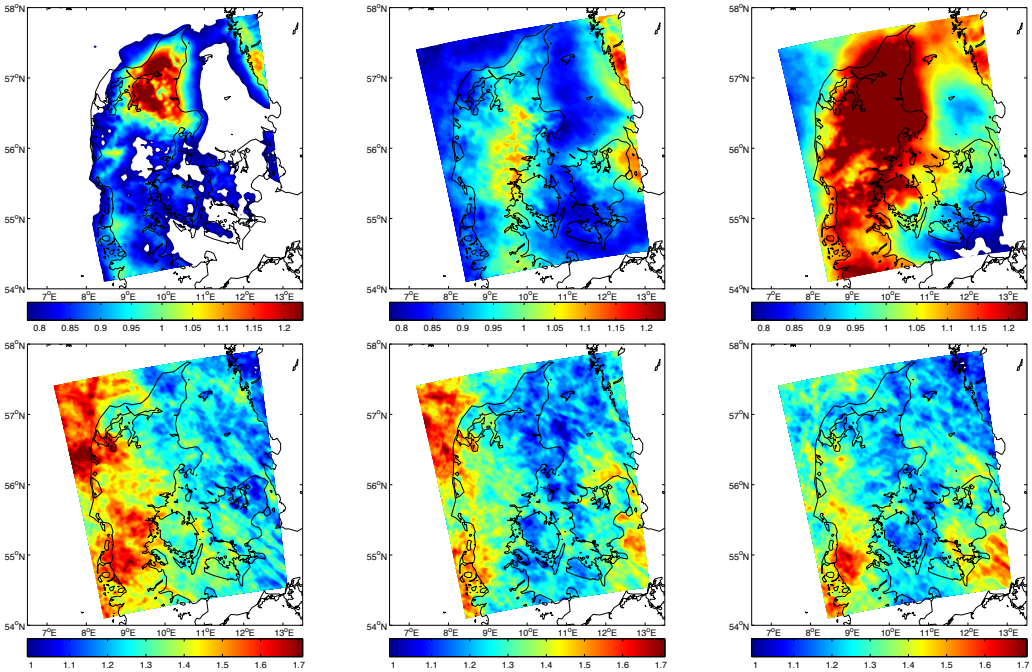

Figure 4: Root mean square differences between the hourly temperature (top) and wind speed (bottom) 2D fields simulated in September 2013 at ≈100 m. The left frames correspond to the difference between the MYJ and the MYNN schemes, the middle between the MYJ and the YSU schemes, and the right between the MYNN and YSU schemes. The colorbars are in K and m s^{-1}

Høvsøre at the west coast of Denmark. Details on the mast and these measurements are given in Sec. 4. Here we compare the wind speeds closest to 100, 40 and 10 m and the temperature at 100 m. Figure 5 illustrates the comparison of simulations and observations for such outputs in terms of their diurnal behavior. The simulated wind speeds show good agreement between them, with no obvious outperformance, all slightly underpredicting the observed values. However, when looking at the temperature comparison, the YSU simulations are clearly much closer to the observations. These results (and some other based on other studies) provide us with confidence in using the YSU scheme for the 30-year reanalysis.

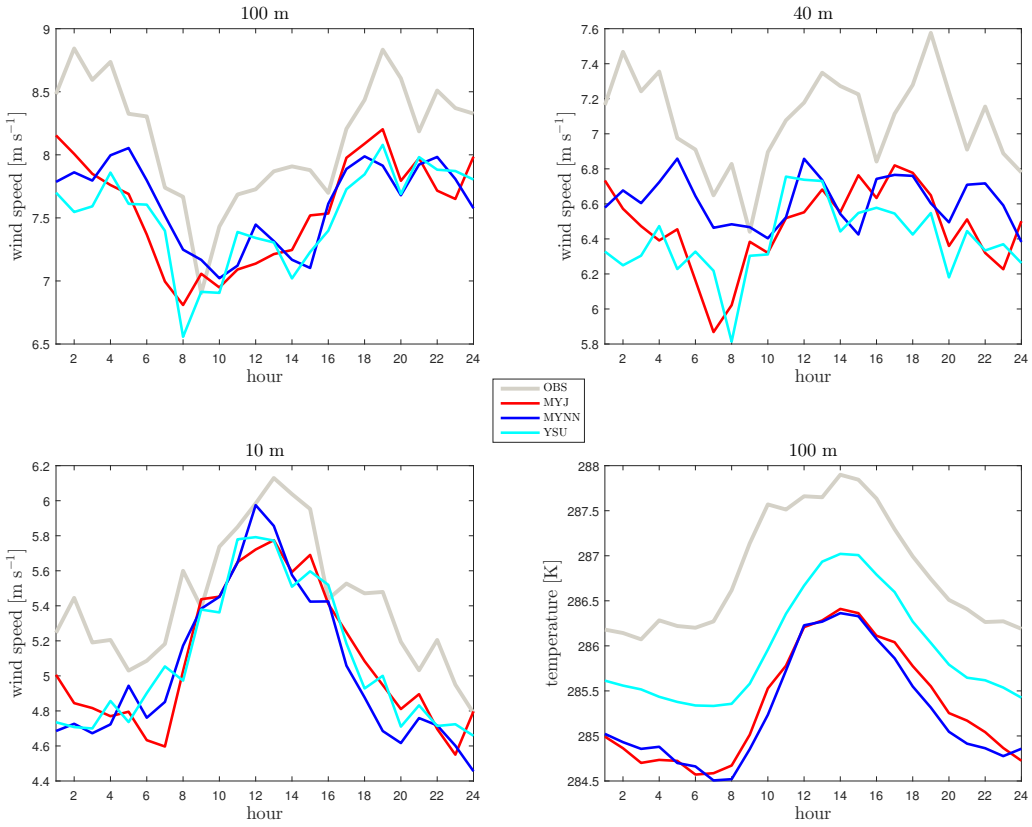

Figure 5: Diurnal behavior of the wind speed and temperature at different levels from the simulations and the observations at Høvsøre

3 Data extraction

KB provided the 'master' Danish register of existing and decommissioned turbines in Denmark valid until March 2014, which contains for each turbine i.a., the registered number of the turbine, the date to which it was connected to the grid, its capacity, rotor diameter, and hub height, and its coordinates in UTM32 Euref89. The register that DTU Wind Energy worked with was scanned, filtered and corrected by KB as some turbine coordinates were obviously wrong.

There were 5196 turbines registered as 'on operation' and 2577 'decommissioned'. Regardless of this, model data were extracted from the day they were connected to the grid until the last day of the simulation (2014-01-09). Figure 6 illustrates a map of Denmark with the 7773 turbine positions.

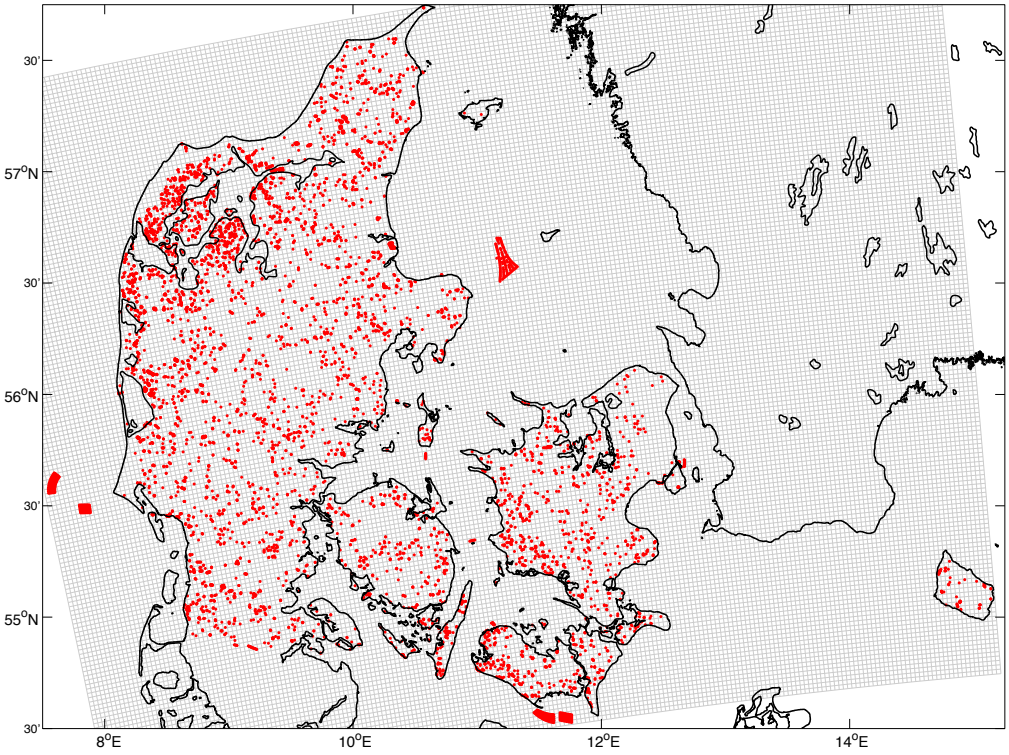

Figure 6: Map with the positions of the registered existing and decommissioned wind turbines in Denmark (in red points). The 2-km mass grid of the WRF model setup used for the simulations (here limited to the minimum and maximum longitude and latitude coordinates where turbines are located) is also shown in grey lines

For each turbine, we extracted meteorological variables (i.e., mean hourly time series of a number of meteorological parameters) from the nearest grid point to the turbine site. This means that in close-spaced wind turbines and wind farms, some turbines will end up with the same value (if they have the same turbine height). Also for each turbine, we extracted the longitudinal and latitudinal wind speed components from the levels above and below the hub height (which are estimated from the base and perturbation pressure fields and the topographical inputs of the simulations). The 2-m specific humidity, 2-m potential temperature, friction velocity, surface heat flux and 10-m longitudinal and latitudinal wind speed components are also extracted for each turbine positions in order to produce the final dataset delivered to KB.

It was agreed with KB and with DELTA that the data will be delivered as time series with the simulated data in .txt files (each per turbine) with the format shown in Fig. 7. The file name is "WT" followed by the turbine registration number, which is available in the register. The file contains a header with four columns (wind turbine registered number; hub height; UTM East-

ing; UTM Northing) followed by data distributed in six columns: timestamp; wind speed at hub height; direction a hub height; 2-m temperature; 2-m relative humidity; Obukhov length (see Sec. 4 for a better description of the output data).

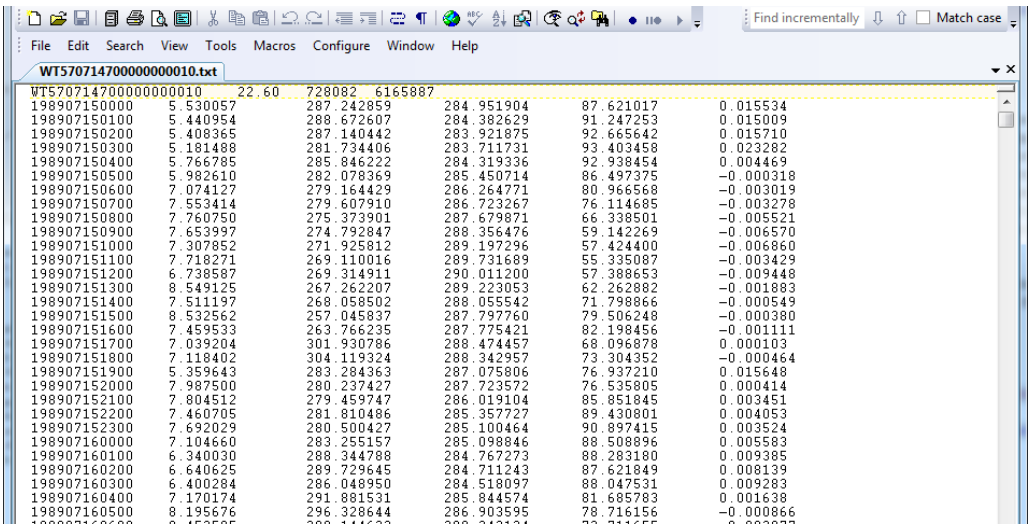

Figure 7: Format of each of the files delivered to KB with the simulated meteorological data

4 Model evaluation

Evaluation of a number of model simulation outputs is performed by comparison with measurements from the high-quality met mast DTU Wind Energy runs at the National Test Station for Wind Turbines at Høvsøre, Denmark. The mast and the site are described in detail in Peña et al. (2015).

For the evaluation at Høvsøre we extracted WRF output data corresponding to the grid point closest to the mast location (see Fig. 8). This point is not only the closest but perhaps most 'similar' grid point in the mast location neighborhood as the distance from it to the closest strong roughness change (in this case from water to land, which in the region is the feature with higher impact on the wind flow) is nearly the same as that from the mast to the west coast (as westerly winds are predominant at Høvsøre).

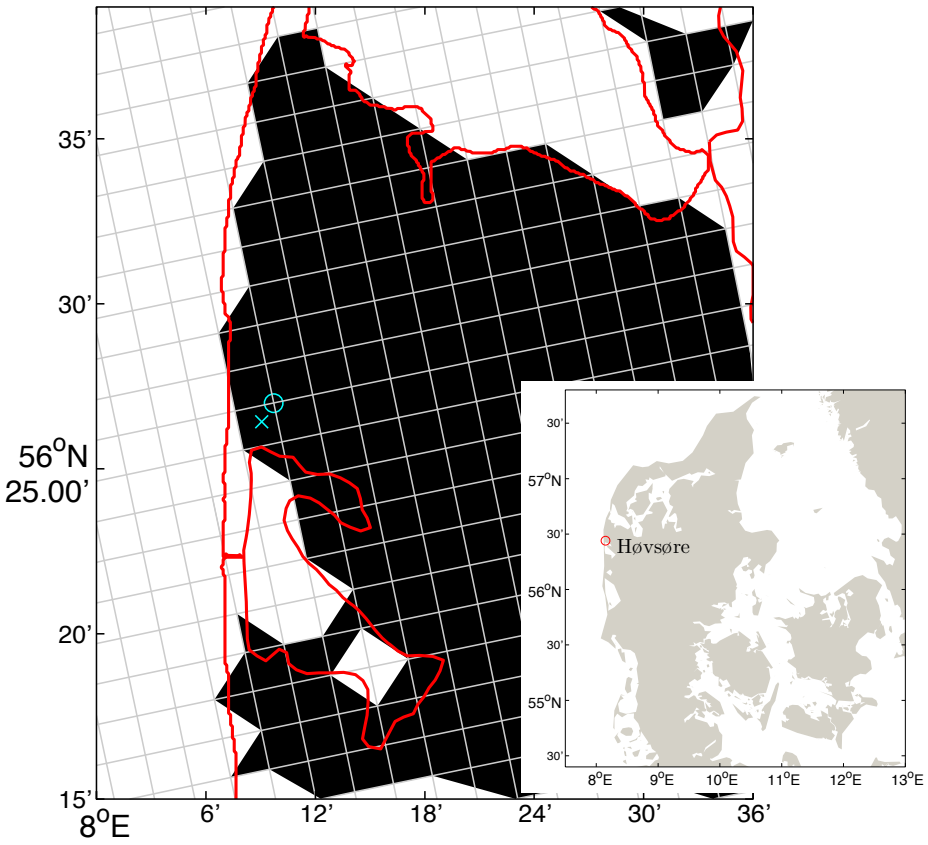

Figure 8: The location of the Høvsøre meteorological mast in Denmark. The location of the mast (cross) and that of the grid point closest to it (circle) are shown in cyan. The model horizontal grid is also shown in grey lines as well as the land mask in black. The location of Høvsøre in Denmark is illustrated in the bottom right of the figure

The met mast at Høvsøre is heavily equipped with instrumentation from the soil level up to 116.5 m but here we use measurements from the instruments observing 'equivalent parameters' as those required by KB and that are extracted from the simulations. These are described in Tab. 3. Data started to be recorded at Høvsøre in Feb. 2014 but this evaluation is going to be performed in the period Jan. 2005–Dec.2013 in order to have complete years.

Instrument–measurement	Height [m]
Cup anemometer–wind speed	116.5, 100, 80, 60, 40, and 10
Wind vane–wind direction	100, 60, and 40
Sonic anemometer–kinematic fluxes	20
Temperature humidity sensor–temperature	2
Humidity sensor–relative humidity	2

Table 3: Measurements at the Høvsøre met mast used for mesoscale model evaluation

4.1 Long-term climatology

Figure 9 illustrates the wind climatology[2] at Høvsøre based on the observations and simulations at 100 m for the period 2005-2013. The raw data at Høvsøre are averaged in 10- and 30-min periods but as the simulations are hourly outputs we present (for this case) the 10-min climatology as well (for the rest of the evaluation, the hourly observation is not the hourly average but the 10-min mean, which corresponds to the hourly mesoscale model output).

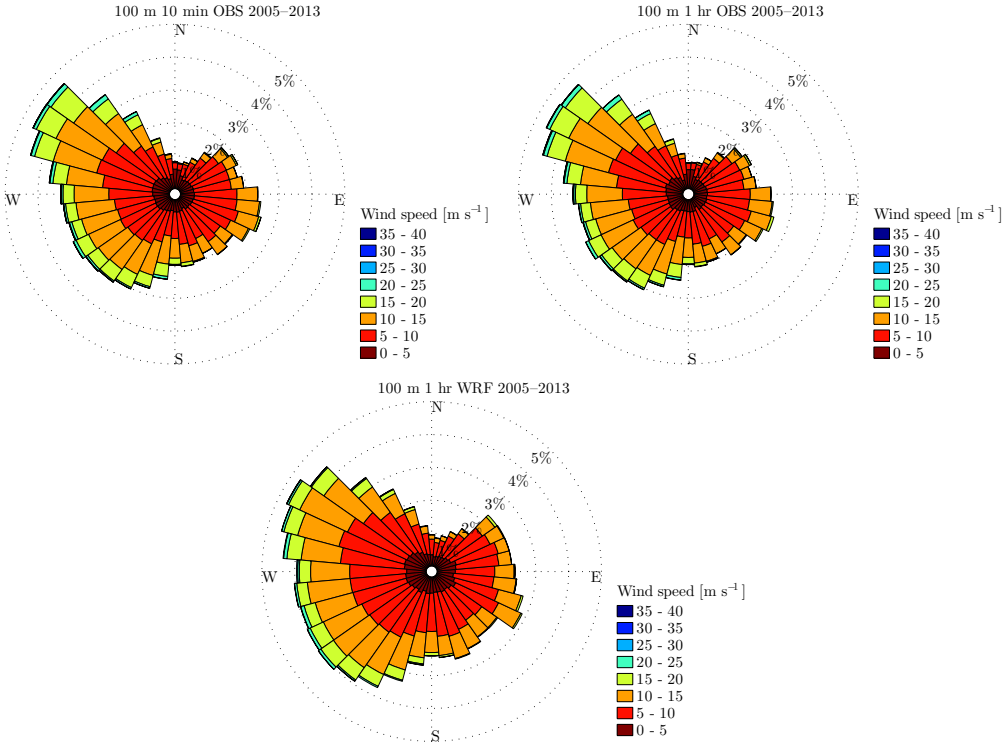

Figure 9: Wind rose climatology at Høvsøre at 100 m. The upper-left frame shows the 10-min observations, the upper-right the 1-hour observations, and the bottom frame the 1-hour simulation output

Common to the three types of climatologies is that they show the same pattern, i.e., predominant winds are northwesterly and a rather high southeasterly component. The simulations are slightly more evenly distributed on the wind sectors being the north, the less frequent one. From the observations the effect of the neighboring turbines is observed as for the north sector, the lowest wind speed range (0–5 m s^{-1}) is the more frequent (there are five large wind turbines in a north-to-south row north of the mast at Høvsøre). Also, it can be seen that the same climatology is observed for the 10-min dataset compared to the 1-hour one.

From recent work (Kelly and Gryning, 2010; Peña and Hahmann, 2012) another "long-term" parameter, namely the long-term stability correction, can also be estimated from observations

[2] generally climatology refers to 50 years but in wind power meteorology it refers to more than 1 year

and simulations in order to better describe the wind conditions of a site. Such a correction is important in order to know the long-term effect of the occurrences of non-neutral conditions in the surface layer; therefore, although the mesoscale model could have difficulties predicting the stability conditions accurately, we expect that the atmospheric stability histograms based on the simulated outputs agree with those from the observations. Most specifically, we would like similar characteristics of the histograms of the Obukhov length L, the stability parameter used for correction of wind speed due to diabatic conditions. This is defined as

$$L = -\frac{\overline{T}\, u_*^3}{\kappa\, g\, \overline{w'T'}}, \tag{1}$$

where $\overline{T}$ is the mean temperature of the air layer, u_* the friction velocity, κ the von Kármán constant ($= 0.4$), g the gravitational acceleration, and $\overline{w'T'}$ the kinematic heat flux. Figure 10 illustrates the histograms of $1/L$ for both the simulations and the observations (neutral conditions are located the closest $1/L$ approaches zero and more negative and positive values denote more unstable and stable atmospheres), which are indeed very similar. Similar results were found from WRF model simulations and observations in the North and Baltic seas (Peña and Hahmann, 2012; Peña et al., 2012).

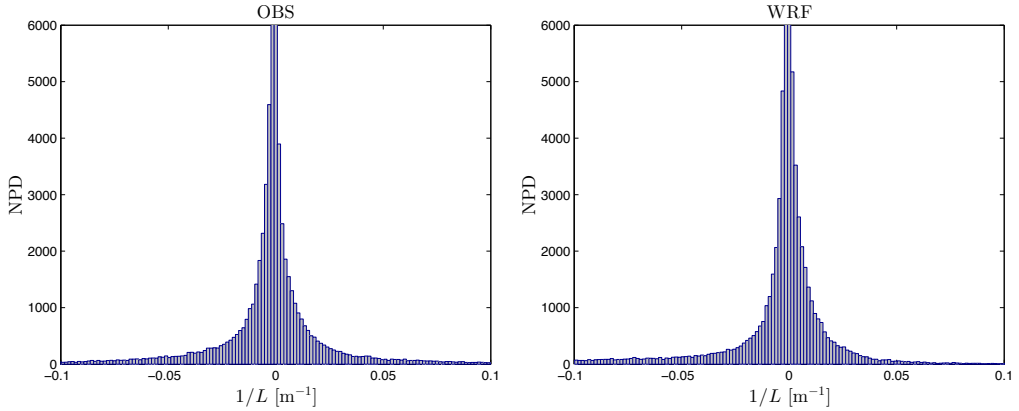

Figure 10: Normalized histograms of $1/L$ from both observations (left) and simulations (right) at Høvsøre

Figure 11 shows the long-term (average) wind profiles from simulations and observations at Høvsøre. As illustrated the simulations underestimate in average the wind speed within the first 125 m. The reason for such underestimation is a combination of different phenomena and numerical approximations. However one can very simplistically explain it based on the value of the roughness used in the model. At Høvsøre this value is 0.1 m, which is almost an order of magnitude higher than the estimated roughness (≈0.015 m) at the site using surface-layer theory (Peña et al., 2015). Assuming that the model is able to predict the geostrophic and large-scale conditions well, then for a site like Høvsøre the major effect of the surface on the boundary-layer winds is via the roughness value; a high value tends to produce lower wind speeds due to the effect of roughness (z_o) on the wind ($\propto 1/z_o$).

There are two very good aspects of the results in Fig. 11. First that both simulations and observations show nearly the same variability. Second that the average wind profile from the simulation shows nearly the same wind shear as that from the observation. This is indeed very interesting as many atmospheric conditions at Høvsøre are either stable or very stable with very high wind shears and these type of situations are very difficult to reproduce by the model (Hu et al., 2010).

4.2 Scatter plots

Figure 12 shows scatter plots of the observed and simulated hourly wind speed and direction at 100 m; u and v are the two horizontal wind speed components (the former is the longitudinal and

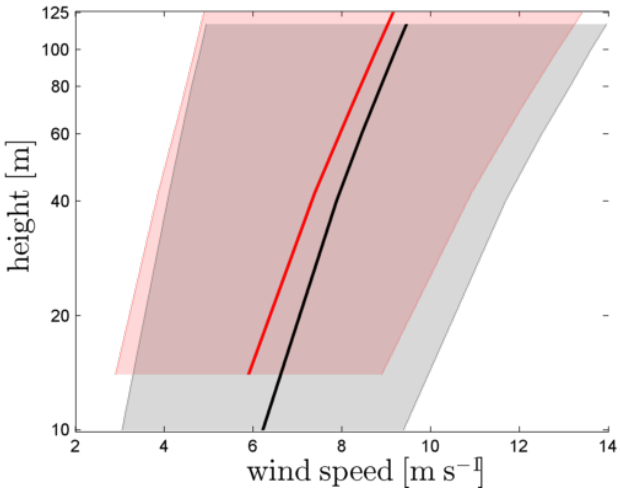

Figure 11: Wind profile climatology at Høvsøre from simulations (red) and observations (black). The mean is represented by the solid line and the filled area ±one standard deviation

the latter the latitudinal) and $U = \sqrt{u^2 + v^2}$. As illustrated, the model is able to simulate rather well both wind speed components when compared to the observations. The correlation with measurements is high (Pearson's linear correlation ≈ 0.9) for both components and higher compared to previous simulations at Høvsøre (Perez-Andujar, 2013). The wind speed is slightly underpredicted by the simulations, as expected from the results in Fig. 11, and in the wind direction there is good agreement between the simulations and observations.

4.3 Diurnal behavior

In a mesoscale reanalysis one important (perhaps the most important) feature of the simulated parameters is that they should be able to represent the variability of the atmospheric conditions well and one way to evaluate their representative is by looking at their diurnal behavior. Figure 13 illustrates such behavior for the 2-m simulated and observed temperature (T_2) and relative humidity (RH).

As illustrated simulated and observed T_2 and *RH* are in very good agreement, WRF simulations being ≈0.5 K colder and ≈2% more humid than the observations. Close to the surface, colder simulations are typically derived from WRF (Draxl et al., 2014b).

Figure 14 shows a similar exercise but for the observed and simulated surface friction velocity u_* and heat flux $\overline{w'T'}$. These two turbulence parameters are estimated "directly" with the sonic instrument at the mast. However, there are not products of the simulated atmosphere in WRF but derived from parameterizations, like those which are the base of Monin-Obukhov similarity theory (Monin and Obukhov, 1954).

Interestingly the simulated friction velocity is much higher than the observed one. This is mainly due to the much higher roughness in the simulations when compared to the observations. For the simulations to 'match' the observed wind speed, the simulated u_* needs to be much higher than the observed one as $U \approx (u_*/\kappa)\ln(z/z_o)$ (in fact the ratio $u_{*\mathrm{WRF}}/u_{*\mathrm{OBS}} \approx \ln(z_{\mathrm{OBS}})/\ln(z_{\mathrm{WRF}})$ predicts well the difference between the two curves in the plot. The surface heat flux, on the other hand, is very well simulated by the WRF model simulations in the mean but it can be seen that the variability observed from the measurements is much confined in the simulations as expected.

Figure 15 shows the diurnal behavior of the inverse of the Obukhov length estimated as in Eq. (1). As illustrated, the simulations show much less variability around the mean, which means that the simulated atmospheric conditions do not frequently become very unstable or stable, whereas this is indeed a phenomenon shown by the observations. Although the character of the observations is to produce a fluctuating behavior for $1/L$, one can see that the observations (and the simulations) are often stable during the night (from about 18:00 to 06:00) and unstable during the day. During daytime, the simulations are in average not that unstable compared to the

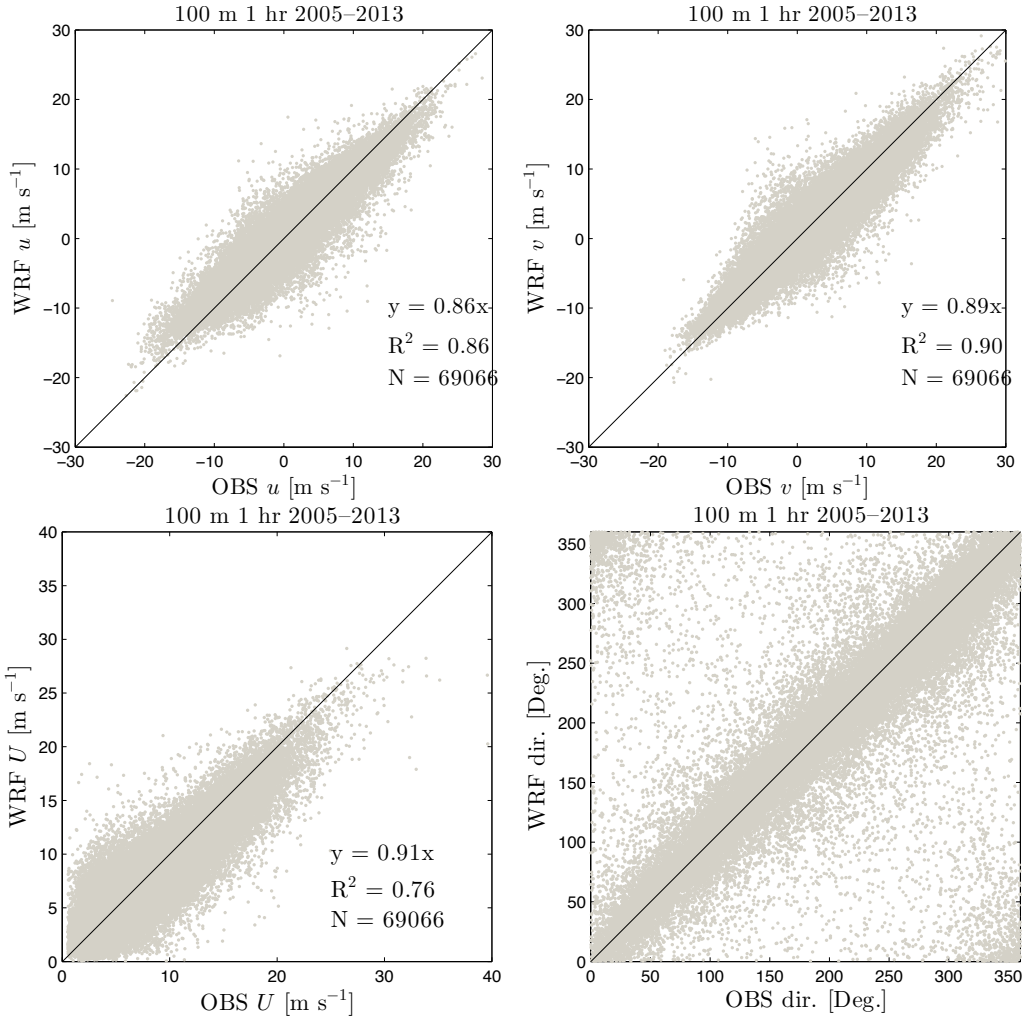

Figure 12: Scatter plots of hourly model simulations and observations of wind speed and direction at 100 m at Høvsøre: u wind speed component (upper-left frame), v wind speed component (upper-right frame), mean wind speed component (bottom-left frame), and direction (bottom-right frame)

observations and during nighttime after sunset not that stable either.

Finally, figure 16 illustrates the diurnal of the wind speed at several heights at the met mast and the closest/equivalent WRF levels. Close to the surface (from both simulations and observations) the effect of the surface is very clear from a wind speed peak in the afternoon. The peak diminishes with height very similarly in both simulations and observations and at 116 m the wind speed does not seem to vary much as at this height the marine characteristics are much clearer and as shown in Peña et al. (2012) under marine conditions there is no distinguished diurnal behavior in the wind.

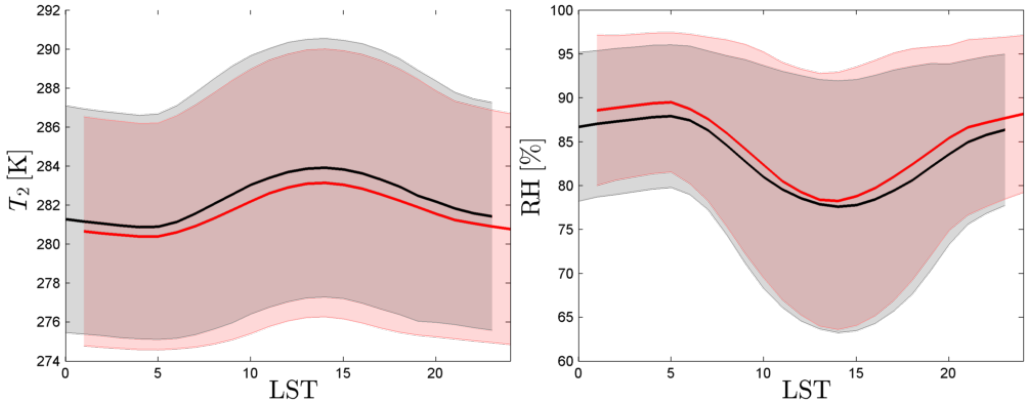

Figure 13: Diurnal behavior of the 2-m temperature (left) and relative humidity (right) from model simulations (red) and observations (black) at Høvsøre. The mean is represented by the solid line and the filled area ±one standard deviation

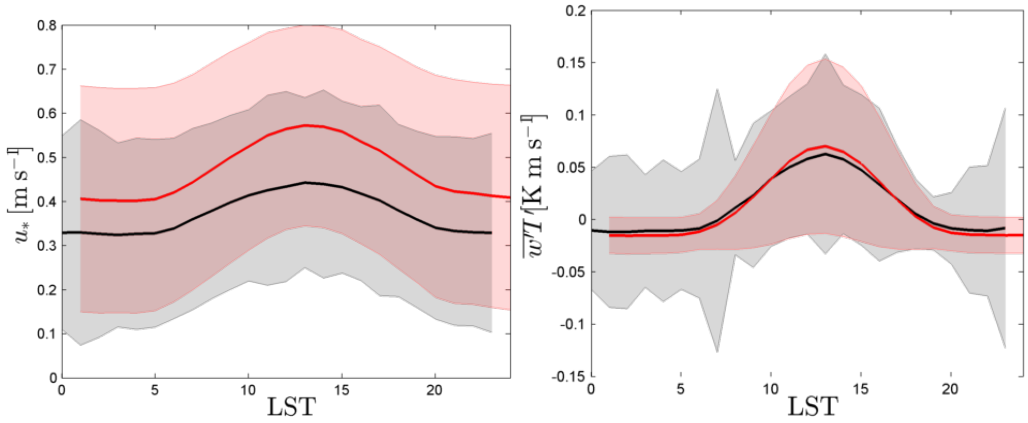

Figure 14: Like Fig. 13 but for the surface friction velocity (left) and heat flux (right)

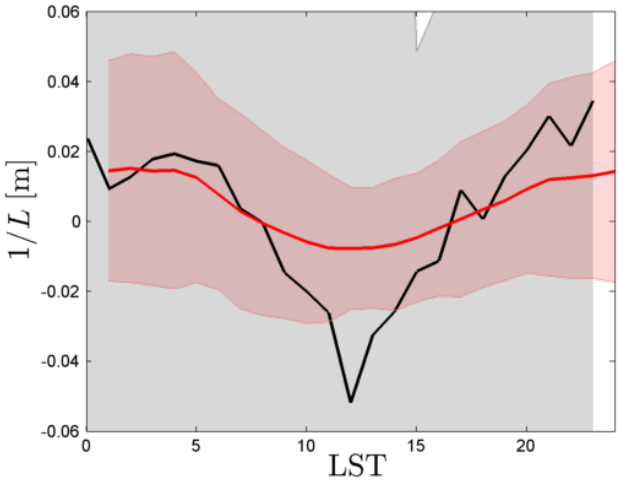

Figure 15: Like Fig. 13 but for the inverse of the Obukhov length

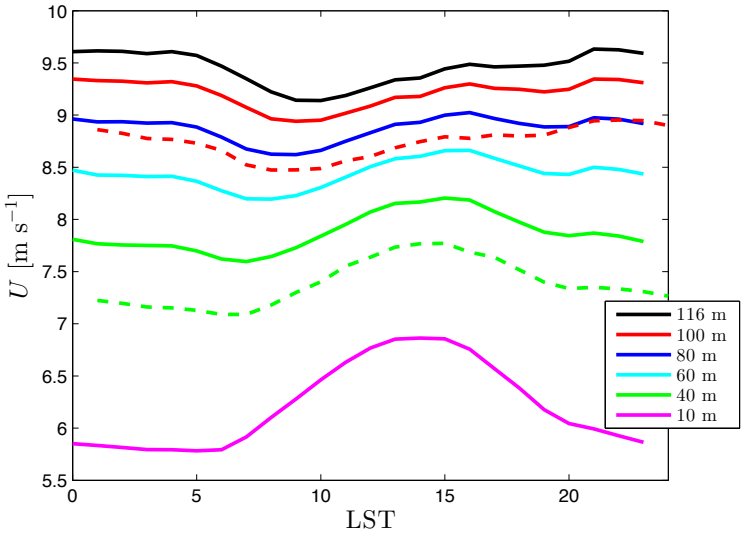

Figure 16: Diurnal behavior of wind speeds at several levels from observations (solid lines) and simulations (dashed lines) at Høvsøre

4.4 Averaged winds over Denmark

Figure 17 shows the WRF-derived mesoscale winds at 100 meters for the last 11 years (2003–2013) of the simulations.

4.5 Other potential sources of error

Possible sources of errors in the wind speed data can be related to

- No verification against measured wind speeds was undertaken here. But, from previous studies (Hahmann and Peña, 2010) we find that the verification against 10-meter winds shows positive biases (i.e., simulated wind speeds are larger than those observed) at night over most inland stations.
- The mesoscale model smooths the gradients in wind speeds along the coastlines, thus uncertainties there are larger than in more homogeneous inland locations.
- The are uncertainties in the global atmospheric data and sea surface temperatures used to drive the mesoscale model
- Changes in land use and land cover (e.g. urban areas) have been included as averaged in the period 2001-2010. Therefore, changes in surface land cover within the 30 years of the simulations have not been taken into account.

5 Summary

We have provided KB with a high-quality dataset of WRF model simulation outputs for 7773 wind turbine locations throughout Denmark. The simulations were performed during 30 years and the data delivered to KB contain the simulated wind speed and direction at hub height, 2-meter temperature, 2-meter relative humidity and a measure of the atmospheric stability close to the ground.

We performed a sensitivity analysis on the entire Denmark to determine the setup of the WRF model regarding PBL schemes and an evaluation of the simulations from model pre-runs with high-quality observations from a mast at Høvsøre, Denmark. From these analyses, the YSU scheme slightly outperformed the other two PBL schemes evaluated and, therefore, was chosen for the final simulation runs.

Finally, we performed model evaluation of the 30-year run with the concurrent 8 years of observations at Høvsøre. Both modeled and observed wind climatologies show the same pattern with predominant winds from northwest and a high southeast component. Distributions of atmospheric stability are very similar between the model and the observations, providing us confidence on the long-term capabilities of the simulations. The wind profile climatology at Høvsøre is also very close between model and observations, as well as the wind variability. The diurnal behavior of the simulated temperature, relative humidity, and heat flux close to the ground is in very good agreement with that observed at Høvsøre. Wind speeds are slightly underestimated by the model at Høvsøre, partly due to the high roughness length value that the model uses at this location.

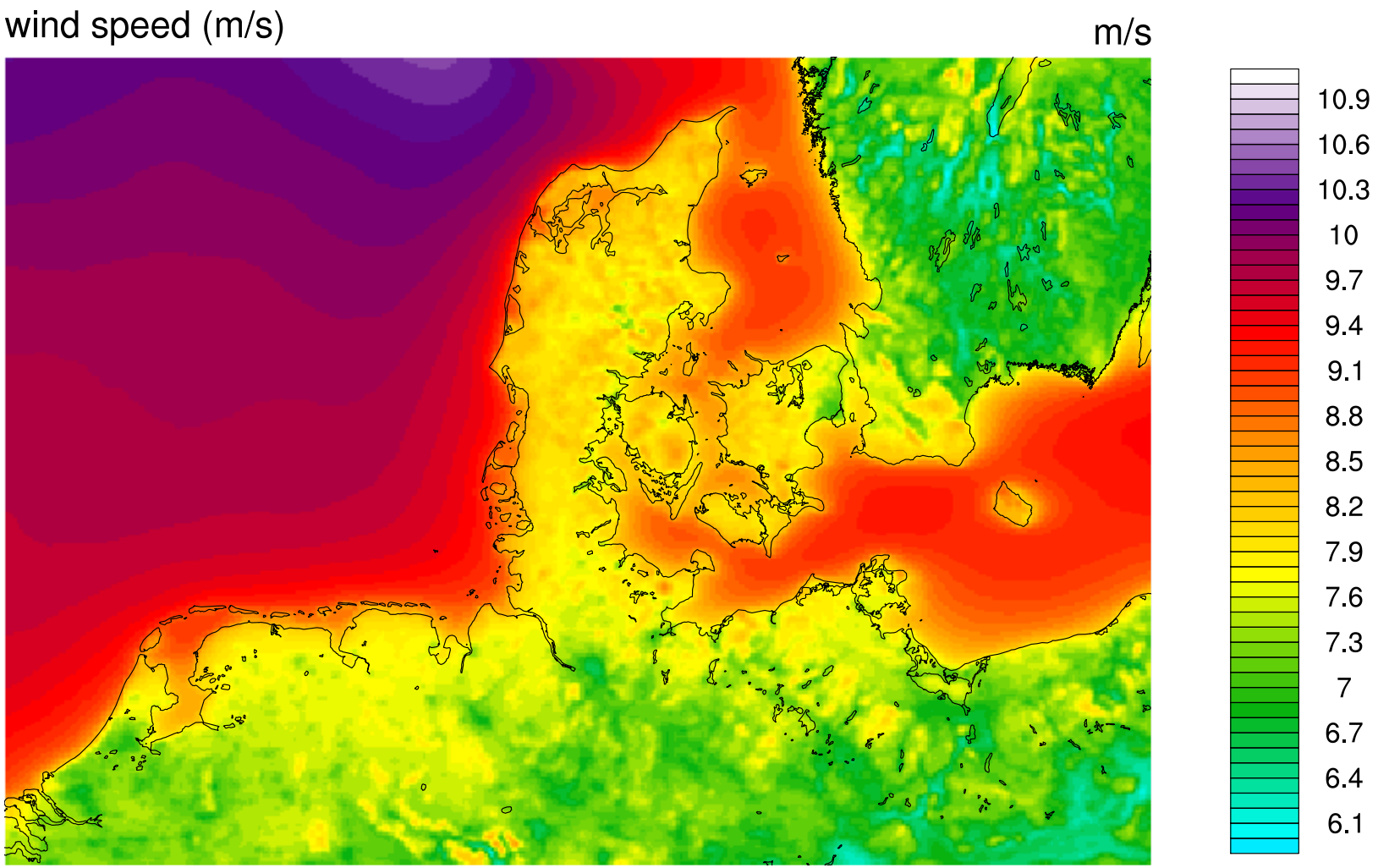

Figure 17: Long-term (2003–2013) averaged wind speed (m/s) at 100 meters derived from the WRF simulations.

References

Dee, D. P., Uppala, S. M., Simmons, A. J., Berrisford, P., Poli, P., Kobayashi, S., Andrae, U., Balmaseda, M. A., Balsamo, G., Bauer, P., Bechtold, P., Beljaars, A. C. M., van de Berg, L., Bidlot, J., Bormann, N., Delsol, C., Dragani, R., Fuentes, M., Geer, A. J., Haimberger, L., Healy, S. B., Hersbach, H., Holm, E. V., Isaksen, L., Kallberg, P., Koehler, M., Matricardi, M., McNally, A. P., Monge-Sanz, B. M., Morcrette, J. J., Park, B. K., Peubey, C., de Rosnay, P., Tavolato, C., Thepaut, J. N., and Vitart, F. (2011). The ERA-Interim reanalysis: configuration and performance of the data assimilation system. *Q. J. R. Meteorolog. Soc.*, 137(656, Part A):553–597.

Draxl, C., Hahmann, A. N., Peña, A., and Giebel, G. (2014a). Evaluating winds and vertical wind shear from WRF model forecasts using seven PBL schemes. *Wind Energy*, 17:39–55.

Draxl, C., Hahmann, A. N., Peña, A., and Giebel, G. (2014b). Evaluating winds and vertical wind shear from Weather Research and Forecasting model forecasts using seven planetary boundary layer schemes. *Wind Energy*, 17:39–55.

Friedl, M. A., Sulla-Menashe, D., Tan, B., Schneider, A., Ramankutty, N., Sibley, A., and Huang, X. (2010). MODIS Collection 5 global land cover: Algorithm refinements and characterization of new datasets. *Remote Sens. Environ.*, 114(1):168–182.

Hahmann, A. N., Badger, J., Vincent, C. L., Kelly, M. C., Volker, P. J. H., and Refslund, J. (2014). Mesoscale modeling for the wind atlas for South Africa (WASA) Project. Technical report, DTU Wind Energy.

Hahmann, A. N. and Peña, A. (2010). Validation of boundary-layer winds from WRF mesoscale forecasts over Denmark. In *European Wind Energy Conference and Exhibition*, Warsaw, Poland.

Hahmann, A. N. and Peña, A. (2010). Validation of boundary-layer winds from WRF mesoscale forecasts over Denmark. In *Proceedings of the European Wind Energy Association Conference & Exhibition*, Warsaw.

Hahmann, A. N., Rostkier-Edelstein, D., Warner, T. T., Vandenberghe, F., Liu, Y., Babarsky, R., and Swerdlin, S. P. (2010). A Reanalysis System for the Generation of Mesoscale Climatographies. *J. Appl. Meteor. Clim.*, 49(5):954–972.

Hong, S.-Y., Noh, Y., and Dudhia. (2006). A new vertical diffusion package with an explicit treatment of entrainment processes. *Mon. Wea. Rev.*, 134:2318–2341.

Hu, X.-M., Nielsen-Gammon, J. W., and Zhang, F. (2010). Evaluation of three planetary boundary layer schemes in the WRF model. *J. Appl. Meteorol. Climatol.*, 49:1831–1844.

Kelly, M. and Gryning, S.-E. (2010). Long-term wind profiles based on similarity theory. *Boundary-Layer Meteorol.*, 136:377–390.

Monin, A. S. and Obukhov, A. M. (1954). Osnovnye zakonomernosti turbulentnogo peremeshivanija v prizemnom sloe atmosfery (Basic laws of turbulent mixing in the atmosphere near the ground). *Trudy Geofiz. Inst. AN SSSR*, 24(151):163–187.

Peña, A. and Hahmann, A. N. (2012). Atmospheric stability and turbulent fluxes at Horns Rev–an intercomparison of sonic, bulk and WRF model data. *Wind Energy*, 15:717–730.

Peña, A., Mikkelsen, T., Gryning, S.-E., Hasager, C. B., , Hahmann, A., Badger, M., Karagali, I., and Courtney, M. (2012). *Offshore vertical wind shear: Final report on NORSEWInD work task 3.1*. DTU Wind Energy-E-Report-0005(EN). DTU Wind Energy.

Perez-Andujar, A. (2013). Long-term corrections for wind resource assessment. Technical Report Master-Series-M-0047(EN), DTU Wind Energy.

Peña, A., Floors, R., Wagner, R., Courtney, M. S., Gryning, S.-E., Sathe, A., Larsén, X. G., Hahmann, A. N., and Hasager, C. B. (2015). Ten years of boundary-layer and wind-power meteorology at Høvsøre, Denmark. *Boundary-Layer Meteorol.* in press.

Refslund, J., Dellwik, E., Hahmann, A. N., Barlage, M. J., and Boegh, E. (2014). Development of satellite green vegetation fraction time series for use in mesoscale modeling: application to the European heat wave 2006. *Theor. Appl. Climatol.*, 117(3-4 (August)):377–392.

Reynolds, R. W., Gentemann, C. L., and Corlett, G. K. (2010). Evaluation of AATSR and TMI satellite SST data. *J. Climate*, 23(1):152–165.

DTU Wind Energy
Technical University of Denmark

Frederiksborgvej 399
4000 Roskilde
Denmark
Phone +45 4677 5024

www.vindenergi.dtu.dk